Chinese Journal of Physiology 57(1): 31-40, 2014
DOI: 10.4077/CJP.2014.BAB141

Rise of $[Ca^{2+}]_i$ and Apoptosis Induced by *M*-3M3FBS in SCM1 Human Gastric Cancer Cells

Wei-Chuan Chen[1], Chiang-Ting Chou[2, 3], Wen-Chin Liou[1], Shiuh-Inn Liu[4], Ko-Long Lin[5], Ti Lu[6], Yi-Chau Lu[7], Shu-Shong Hsu[4], Jeng-Yu Tsai[4], Wei-Chuan Liao[4], Wei-Zhe Liang[8], and Chung-Ren Jan[8]

[1]*Department of Surgery, St. Joseph Hospital, Kaohsiung 80288*
[2]*Department of Nursing, Division of Basic Medical Sciences, Chang Gung University of Science and Technology, Chia-Yi 61363*
[3]*Chronic Diseases and Health Promotion Research Center, Chang Gung University of Science and Technology, Chia-Yi 61363*
[4]*Department of Surgery, Kaohsiung Veterans General Hospital, Kaohsiung 81362*
[5]*Department of Rehabilitation, Kaohsiung Veterans General Hospital, Kaohsiung 81362*
[6]*Department of Psychiatry, Kaohsiung Veterans General Hospital, Kaohsiung 81362*
[7]*Department of Orthopedics, Kaohsiung Veterans General Hospital, Kaohsiung 81362*
and
[8]*Department of Medical Education and Research, Kaohsiung Veterans General Hospital Kaohsiung 81362, Taiwan, Republic of China*

Abstract

***M*-3M3FBS (2,4,6-trimethyl-N-(meta-3-trifluoromethyl-phenyl)-benzenesulfonamide is a presumed phospholipase C activator which induced Ca^{2+} movement and apoptosis in different cell models. However, the effect of *m*-3M3FBS on cytosolic free Ca^{2+} concentrations ($[Ca^{2+}]_i$) and apoptosis in SCM1 human gastric cancer cells is unclear. This study explored whether *m*-3M3FBS elevated basal $[Ca^{2+}]_i$ levels in suspended cells by using fura-2 as a Ca^{2+}-sensitive fluorescent dye. *M*-3M3FBS at concentrations between 5-50 μM increased $[Ca^{2+}]_i$ in a concentration-dependent manner. The Ca^{2+} signal was reduced by half by removing extracellular Ca^{2+}. *M*-3M3FBS-induced Ca^{2+} influx was inhibited by nifedipine, econazole, SK&F96365, aristolochic acid, and GF109203X. In Ca^{2+}-free medium, 50 μM *m*-3M3FBS pretreatment inhibited the $[Ca^{2+}]_i$ rise induced by the endoplasmic reticulum Ca^{2+} pump inhibitor thapsigargin. Conversely, pretreatment with thapsigargin partly reduced *m*-3M3FBS-induced $[Ca^{2+}]_i$ rise. Suppression of inositol 1,4,5-trisphosphate production with U73122 did not change *m*-3M3FBS-induced $[Ca^{2+}]_i$ rise. At concentrations between 25 and 50 μM *m*-3M3FBS killed cells in a concentration-dependent manner. The cytotoxic effect of *m*-3M3FBS was not reversed by prechelating cytosolic Ca^{2+} with acetoxy-methyl ester of bis-(o-aminophenoxy)-ethane-N,N,N',N'-tetraacetic acid (BAPTA/AM). Annexin V/propidium iodide staining data suggest that *m*-3M3FBS induced apoptosis at 25 and 50 μM. *M*-3M3FBS also increased levels of superoxide. Together, in human gastric cancer cells, *m*-3M3FBS induced a $[Ca^{2+}]_i$ rise by inducing phospholipase C-independent Ca^{2+} release from the endoplasmic reticulum and Ca^{2+} entry *via* protein kinase C-sensitive store-operated Ca^{2+} channels. *M*-3M3FBS induced cell death that might involve apoptosis *via* reactive oxygen species production.**

Key Words: apoptosis, Ca^{2+}, *m*-3M3FBS, SCM1

Corresponding author: Dr. Chung-Ren Jan, Department of Medical Education and Research, Kaohsiung Veterans General Hospital, Kaohsiung 81362, Taiwan, R.O.C. Tel: +886-7-3422121 ext. 1509, Fax: +886-7-3468056, E-mail: crjan@isca.vghks.gov.tw
Received: July 25, 2012; Revised: September 19, 2012; Accepted: September 24, 2012.
©2014 by The Chinese Physiological Society and Airiti Press Inc. ISSN : 0304-4920. http://www.cps.org.tw

Introduction

Selective activators of phospholipase C (PLC) are still lacking. Bae *et al*. reported a compound 2,4,6-trimethyl-N-(meta-3-trifluoromethyl-phenyl)-benzenesulfonamide (*m*-3M3FBS) that directly stimulates PLC activity (1). Subsequently, *m*-3M3FBS was used as a selective PLC activator in different models such as neutrophil (5), rat mesenteric artery (23), rat aorta (19). However, caution should be applied because in SH-SY5Y human neuroblastoma cells, it was found that *m*-3M3FBS changed Ca^{2+} movement without activation of PLC (20). Dwyer *et al*. (12) also showed PLC-independent effects of *m*-3M3FBS in murine colon. Thus evidence suggests that *m*-3M3FBS should not be used as a selective PLC activator.

A rise in $[Ca^{2+}]_i$ is a crucial signal for many biological responses in most cells (4, 7-9). However, a uncontrolled $[Ca^{2+}]_i$ rise may lead to abnormality of proliferation, secretion, channel activity, protein dysfunction, apoptosis, and necrosis, *etc* (11, 17). *M*-3M3FBS has been shown to increase $[Ca^{2+}]_i$ and cause death in different cell types susch as human oral cancer cells (10), human prostate cancer cells (29), and canine renal tubular cells (13). Jung *et al*. (18) show that *m*-3M3FBS induces apoptosis in human renal Caki cancer cells through caspase activation, down-regulation of XIAP and Ca^{2+} signaling. It appears that the mechanisms underlying *m*-3M3FBS-induced $[Ca^{2+}]_i$ rise and death vary among cell types.

The goal of this study was to investigate the effect of *m*-3M3FBS on $[Ca^{2+}]_i$, viability, apoptosis, and reactive oxygen species (ROS) production in SCM1 human gastric cancer cells. The effect of *m*-3M3FBS on gastric cells is unknown. This cell line is a useful model for human gastric cell research. Liu *et al*. (22) show that thimerosal-induced apoptosis in SCM1 gastric cancer cells involved activation of p38 Mitogen activated protein (MAP) kinase and caspase-3 pathways.

Fura-2 was applied as a fluorescent Ca^{2+}-sensitive probe to measure $[Ca^{2+}]_i$. The effect of *m*-3M3FBS on $[Ca^{2+}]_i$ rises both in the presence and absence of extracellular Ca^{2+}, the concentration-response relationship, the pathways underlying Ca^{2+} influx and Ca^{2+} release, the internal Ca^{2+} stores, and the role of PLC were examined. The effect of *m*-3M3FBS on viability, apoptosis, and ROS production was explored.

Materials and Methods

Materials

The reagents for cell culture were from Gibco (Gaithersburg, MD, USA). Other reagents were from Sigma-Aldrich (St. Louis, MO, USA).

Cell Culture

SCM1 human gastric cells purchased from Bioresource Collection and Research Center (Taiwan) were cultured in F-12K medium supplemented with 10% heat-inactivated fetal bovine serum, 100 U/ml penicillin and 100 μg/ml streptomycin.

Solutions Used in $[Ca^{2+}]_i$ Measurements

Ca^{2+}-containing medium (pH 7.4) contained 140 mM NaCl, 5 mM KCl, 1 mM $MgCl_2$, 2 mM $CaCl_2$, 10 mM Hepes, and 5 mM glucose. Ca^{2+}-free medium (pH 7.4) contained 140 mM NaCl, 5 mM KCl, 3 mM $MgCl_2$, 0.3 mM EGTA, 10 mM HEPES, and 5 mM glucose. *M*-3M3FBS was dissolved in dimethyl sulfoxide as a 1 M stock solution. The other agents were dissolved in water, ethanol or dimethyl sulfoxide. The concentration of organic solvents in the solution used in experiments did not exceed 0.1%, and did not alter viability or basal $[Ca^{2+}]_i$.

$[Ca^{2+}]_i$ Measurements

Confluent cells grown on 6 cm dishes were trypsinized and made into a suspension in culture medium at a density of 10^6/ml. Cells were subsequently loaded with 2 μM fura-2/AM for 30 min at 25°C in the same medium. After loading, cells were washed with Ca^{2+}-containing medium twice and were resuspended in Ca^{2+}-containing medium at a density of 10^7/ml. Fura-2 fluorescence measurements were performed in a water-jacketed cuvette (25°C) with continuous stirring; the cuvette contained 1 ml of medium and 0.5 million cells. Fluorescence was monitored with a Shimadzu RF-5301PC spectrofluorophotometer immediately after 0.1 ml cell suspension was added to 0.9 ml Ca^{2+}-containing or Ca^{2+}-free medium, by recording excitation signals at 340 nm and 380 nm and emission signal at 510 nm at 1-sec intervals. During the recording, reagents were added to the cuvette by pausing the recording for 2 sec to open and close the cuvette-containing chamber. For calibration of $[Ca^{2+}]_i$, after completion of the experiments, the detergent Triton X-100 and 5 mM $CaCl_2$ were added to the cuvette to obtain the maximal fura-2 fluorescence. Then the Ca^{2+} chelator EGTA (10 mM) was subsequently added to chelate Ca^{2+} in the cuvette to obtain the minimum fura-2 fluorescence. $[Ca^{2+}]_i$ was calculated as previously described (16).

Cell Viability Assays

The measurement of cell viability was based on

the ability of cells to cleave tetrazolium salts by dehydrogenases. Augmentation in the amount of developed color directly correlated with the number of live cells. Assays were performed according to manufacturer's instructions designed specifically for this assay (Roche Molecular Biochemical, Indianapolis, IN, USA). Cells were seeded in 96-well plates at a density of 10,000 cells/well in culture medium for 24 h in the presence of 0-50 μM *m*-3M3FBS. The cell viability detecting reagent 4-[3-[4-Iodophenyl]-2-4(4-nitrophenyl)-2H-5-tetrazolio-1, 3-benzene disulfonate] (WST-1; 10 μM pure solution) was added to samples after *m*-3M3FBS treatment, and cells were incubated for 30 min in a humidified atmosphere. In experiments using BAPTA/AM to chelate cytosolic Ca^{2+}, cells were treated with 5 μM BAPTA/AM for 1 h prior to incubation with *m*-3M3FBS. The cells were washed once with Ca^{2+}-containing medium and incubated with or without *m*-3M3FBS for 24 h. The absorbance of samples (A_{450}) was determined using enzyme-linked immunosorbent assay (ELISA) reader. Absolute optical density was normalized to the absorbance of unstimulated cells in each plate and expressed as a percentage of the control value.

Alexa ®Flour 488 Annexin V/Propidium Iodide (PI) Staining for Apoptosis

Annexin V/PI staining assay was employed to further detect cells in early apoptotic and late apoptotic/necrotic stages. Cells were exposed to *m*-3M3FBS at concentrations of 0, 25 μM, or 50 μM for 24 h. Cells were harvested after incubation and washed in cold phosphate-buffered saline (PBS). Cells were resuspended in 400 μl reaction solution with 10 mM of HEPES, 140 mM of NaC1, 2.5 mM of $CaC1_2$ (pH 7.4). Alexa Fluor 488 annexin V/PI staining solution (Probes Invitrogen, Eugene, OR, USA) was added in the dark. After incubation for 15 min, the cells were collected and analyzed in a FACScan flow cytometry analyzer. Excitation wavelength was at 488 nm and the emitted green fluorescence of Annexin V (FL1) and red fluorescence of PI (FL2) were collected using 530 nm and 575 nm band pass filters, respectively. A total of 20,000 cells were analyzed per sample. Light scatter was measured on a linear scale of 1024 channels and fluorescence intensity was on a logarithmic scale. The amount of early apoptosis and late apoptosis/necrosis were determined, respectively, as the percentage of Annexin V^+/PI^- or Annexin V^+/PI^+ cells. Data were later analyzed using the flow cytometry analysis software WinMDI 2.8 (by Joe Trotter, freely distributed software). X and Y coordinates refer to the intensity of fluorescence of Annexin and PI, respectively.

Detection of Intracellular ROS by Flow Cytometry

Cells were plated in triplicate at a density of 2×10^5 cells/well in 6-well plates (Falcon, BD Biosciences, Franklin Lakes, NJ, USA). After overnight incubation, cells were treated with several concentrations of *m*-3M3FBS for 24 h. Cells were harvested, washed twice with cold PBS, and then 2′,7′ -dichlorofluorescein diacetate (DCFH-DA) and dihydroethidine (DHE) were added at a final concentration of 50 μg/ml in Ca^{2+}-containing medium. Cells were incubated for 30 min at 37°C. After cells were washed twice with cold PBS, 1 ml cold PBS was added. These two fluorescent probes were commonly used for detection of intracellular oxidants. During an intracellular oxidative burst, ROS species are usually generated, leading to the conversion of the non-fluorescent probes into fluorescent molecules. The oxidation product of DCFH is dichloroflurescein (DCF), with the green emission at 529 nm, while that of DHE is ethidium, emitting red fluorescence at 590 nm with a FACS Calibur flow cytometer (BD Biosciences, Franklin Lakes, NJ, USA). Data were later analyzed using the flow cytometry analysis software WinMDI 2.8 (by Joe Trotter, freely distributed software) by gating 10^2-10^4 areas of the X and Y coordinates.

Statistics

Data are reported as means ± SEM of 3-5 separate experiments. Data were analyzed by two-way analysis of variances (ANOVA) using the Statistical Analysis System (SAS®, SAS Institute Inc., Cary, NC, USA). Multiple comparisons between group means were performed by *post-hoc* analysis using the Tukey's HSD (honestly significantly difference) procedure. A *P*-value less than 0.05 is considered significant.

Results

Fig. 1A shows that the basal $[Ca^{2+}]_i$ level was 51 ± 2 nM. At concentrations between 5 and 50 μM, *m*-3M3FBS evoked $[Ca^{2+}]$i rises in a concentration-dependent manner in Ca^{2+}-containing medium. The $[Ca^{2+}]_i$ rise induced by 50 μM *m*-3M3FBS attained to 270 ± 2 nM followed by a decay. At 1 μM, *m*-3M3FBS did not induce a $[Ca^{2+}]_i$ rise. The Ca^{2+} response saturated at 50 μM *m*-3M3FBS because at a concentration of 60 μM, *m*-3M3FBS induced a similar response as that induced by 50 μM. Fig. 1B shows that in the absence of extracellular Ca^{2+}, 10-50 μM *m*-3M3FBS induced $[Ca^{2+}]_i$ rises in a concentration-dependent manner. At 50 μM, *m*-3M3FBS induced a $[Ca^{2+}]_i$ rise of 88 ± 2 nM followed by a decay. Fig. 1C shows the concentration-response plots of *m*-3M3FBS-

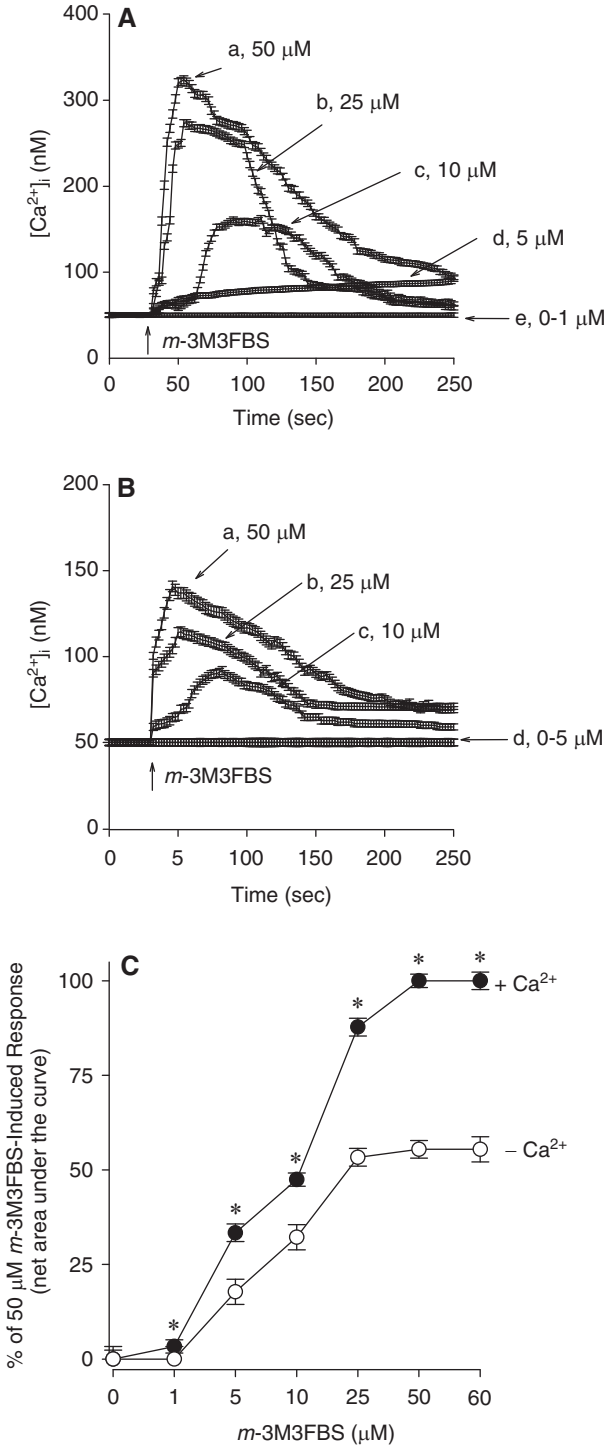

Fig. 1. (A) Effect of *m*-3M3FBS on $[Ca^{2+}]_i$ in fura-2-loaded SCM1 cells. *M*-3M3FBS was added at 25 sec. The concentration of *m*-3M3FBS was indicated. The experiments were performed in Ca^{2+}-containing medium. (B) A concentration-response plot of *m*-3M3FBS-induced Ca^{2+} signals. (C) A concentration-response plot of *m*-3M3FBS-induced $[Ca^{2+}]_i$ rise in the presence of extracellular Ca^{2+}. Y axis is the percentage of control which is the net (baseline subtracted) area under the curve (25-250 sec) of the $[Ca^{2+}]_i$ rise induced by 50 μM *m*-3M3FBS. Data are means ± SEM of three separate experiments.

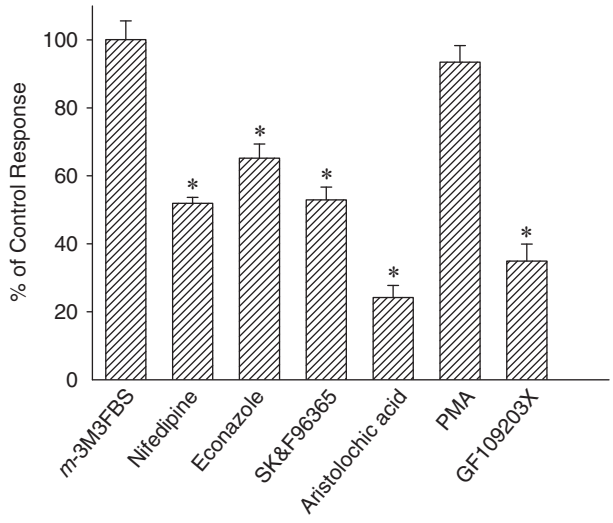

Fig. 2. Effect of Ca^{2+} channel blockers and phospholipase A2 inhibitor on *m*-3M3FBS-induced $[Ca^{2+}]_i$ rise. The experiments were performed in Ca^{2+}-containing medium. The $[Ca^{2+}]_i$ rise induced by 50 μM *m*-3M3FBS was taken as control. In blocker- or modulator-treated groups, the reagent was added 1 min before *m*-3M3FBS. The concentration was 1 μM for nifedipine, 0.5 μM for econazole, 1 μM for SK&F96365; 20 μM for aristolochic acid, 10 nM for phorbol 12-myristate 13-acetate (PMA) and 2 μM for GF109203X. Data are expressed as the percentage of control (1st column) that is the maximum value of 50 μM *m*-3M3FBS-induced $[Ca^{2+}]_i$ rise, and are means ± SEM of three separate experiments. **P* < 0.05 compared to control.

induced responses. The EC50 value was 10 ± 2 or 10 ± 3 μM in the presence or absence of extracellular Ca^{2+} by fitting to a Hill equation.

Experiments were performed to explore the Ca^{2+} entry pathway of *m*-3M3FBS-induced response. The store-operated Ca^{2+} influx inhibitors econazole (0.5 μM) and SK&F96365 (1 μM); the Ca^{2+} channel blocker nifedipine (1 μM), GF109230X (2 μM; a protein kinase C inhibitor) and aristolochic acid (20 μM; a phospholipase A2 inhibitor) partly inhibited 50 μM *m*-3M3FBS-induced $[Ca^{2+}]_i$ rise. In contrast, phorbol 12-myristate 13-acetate (PMA; 10 nM; a protein kinase C activator) had no effect on *m*-3M3FBS-induced $[Ca^{2+}]_i$ rise (Fig. 2).

Previous evidence shows that the endoplasmic reticulum is the major Ca^{2+} store in SCM1 cells (22). Fig. 3A shows that in Ca^{2+}-free medium, addition of *m*-3M3FBS (25 μM) induced a $[Ca^{2+}]_i$ rise of 61 ± 2 nM followed by a decay. Addition of 1 μM thapsigargin (TG), an inhibitor of endoplasmic reticulum Ca^{2+} pumps (27), at 450 sec failed to induce a $[Ca^{2+}]_i$ rise. Fig. 3B shows that TG induced a transient $[Ca^{2+}]_i$ rise of 20 ± 2 nM. *M*-3M3FBS added afterwards induced a $[Ca^{2+}]_i$ rise of 30 ± 2 nM, which was smaller than the

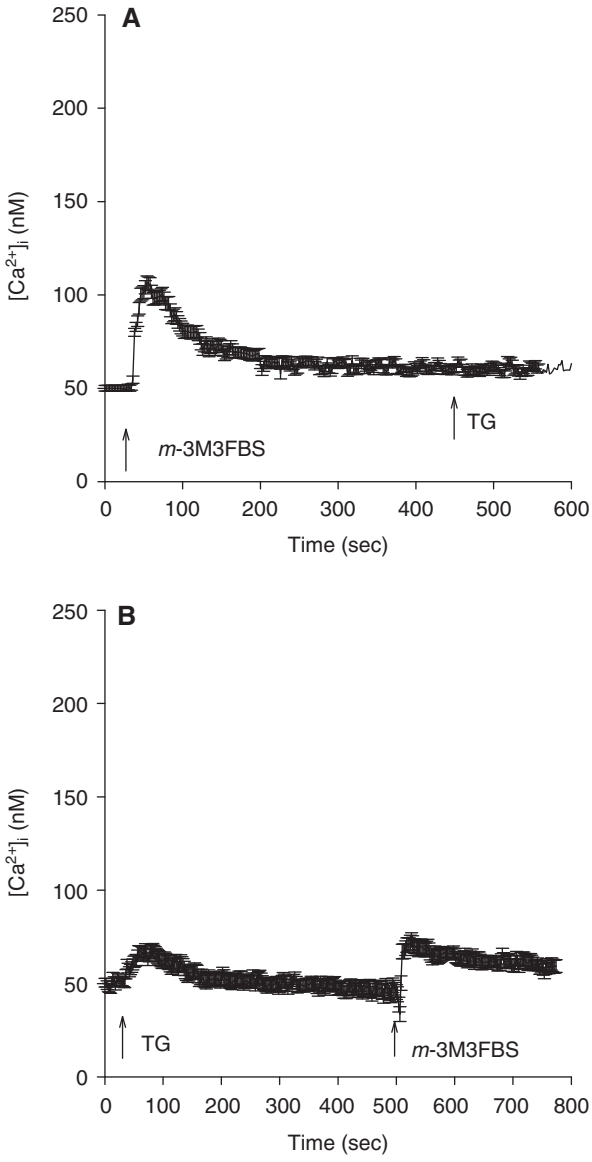

Fig. 3. Intracellular Ca^{2+} stores of *m*-3M3FBS-induced Ca^{2+} release. Experiments were performed in Ca^{2+}-free medium. (A) (B) *M*-3M3FBS (50 μM) and thapsigargin (1 μM) were added at time points indicated. Data are means ± SEM of three separate experiments.

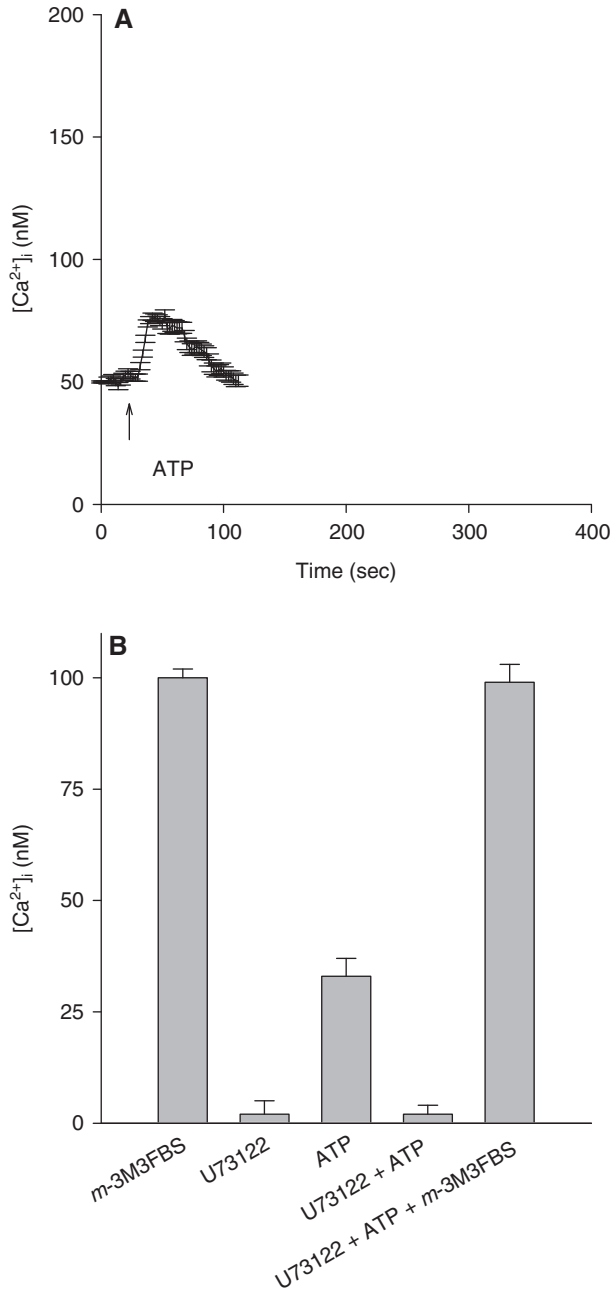

Fig. 4. Lack of effect of U73122 on *m*-3M3FBS-induced Ca^{2+} release. Experiments were performed in Ca^{2+}-free medium. (A) ATP (10 μM) was added as indicated. (B) U73122 (2 μM), ATP (10 μM), and *m*-3M3FBS (50 μM) were added as indicated. Data are means ± SEM of three separate experiments.

m-3M3FBS-induced response in Fig. 3A by 50%.

PLC-dependent formation of inositol 1,4,5-trisphosphate (IP_3) is a crucial step for releasing Ca^{2+} from the endoplasmic reticulum (4). Because *m*-3M3FBS was able to release Ca^{2+} from the endoplasmic reticulum, the role of inositol IP_3 in this release was explored. U73122, an inhibitor of IP_3 formation (28), was applied to see whether IP_3 was required for *m*-3M3FBS-induced Ca^{2+} release. Experiments were first performed to assure that U73122 effectively abolishes production of IP_3. Fig. 4A shows that ATP (10 μM) induced a $[Ca^{2+}]_i$ rise of 31 ± 2 nM. ATP is an IP_3-dependent agonist of $[Ca^{2+}]_i$ rise in most cell types (14). Fig. 4B shows that incubation with 2 μM U73122 did not change basal $[Ca^{2+}]_i$ but abolished ATP-induced $[Ca^{2+}]_i$ rise. This suggests that U73122 effectively suppressed IP_3 production. Fig. 4B also shows that addition of 50 μM *m*-3M3FBS after U73122 and ATP treatments caused a $[Ca^{2+}]_i$ rise not different from control.

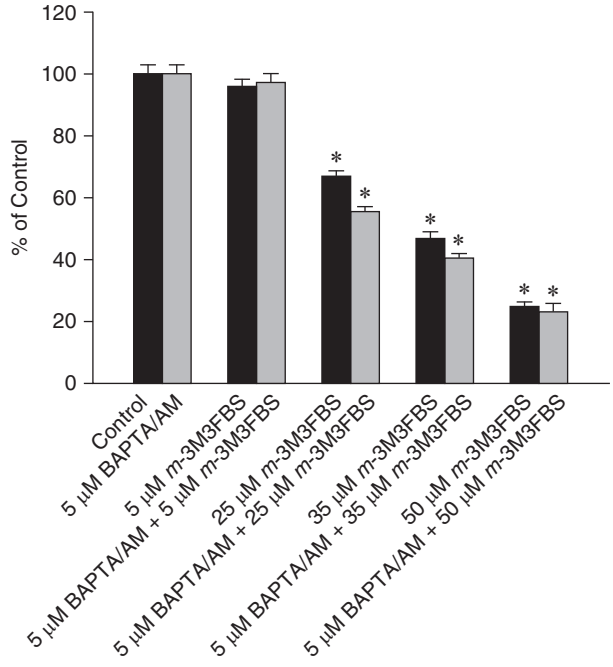

Fig. 5. Cytotoxic effect of *m*-3M3FBS. Cells were treated with 0-40 μM *m*-3M3FBS for 24 h, and the cell viability assay was performed. Data are means ± SEM of three separate experiments. Each treatment had six replicates (wells). Data are expressed as percentage of control response that is the increase in cell numbers in *m*-3M3FBS-free groups. Control had 10,874 ± 215 cells/well before experiments, and had 13,875 ± 814 cells/well after incubation for 24 h. $*P < 0.05$ compared to control. In each group, the Ca^{2+} chelator BAPTA/AM (5 μM) was added to cells followed by treatment with *m*-3M3FBS in medium. Cell viability assay was subsequently performed.

Given that acute incubation with *m*-3M3FBS induced a substantial $[Ca^{2+}]_i$ rise, and that unregulated $[Ca^{2+}]_i$ rises often alter cell viability (4), experiments were performed to examine the effect of *m*-3M3FBS on viability of SCM1 cells. Cells were treated with 0-50 μM *m*-3M3FBS for 24 h, and the tetrazolium assay was performed. In the presence of 5-50 μM *m*-3M3FBS, cell viability decreased in a concentration-dependent manner (Fig. 5).

The next question was whether the *m*-3M3FBS-induced cytotoxicity was related to a preceding $[Ca^{2+}]_i$ rise. The intracellular Ca^{2+} chelator BAPTA/AM (5 μM) (30) was used to prevent a $[Ca^{2+}]_i$ rise during *m*-3M3FBS pretreatment. This BAPTA/AM treatment completely inhibited 50 μM *m*-3M3FBS-induced $[Ca^{2+}]_i$ rise (data not shown). Fig. 5 shows that BAPTA/AM loading did not alter control cell viability. In the presence of 25-50 μM *m*-3M3FBS, BAPTA/AM loading failed to prevent *m*-3M3FBS-induced cell death.

Annexin V/PI staining was applied to detect apoptotic/necrotic cells after *m*-3M3FBS treatment. Figs. 6A and 6B show that treatment with 25 μM or 50 μM *m*-3M3FBS significantly induced apoptosis. At 25 μM, *m*-3M3FBS also induced necrosis. ROS are associated with multiple cellular functions such as cell proliferation, differentiation, and apoptosis (4). To investigate whether *m*-3M3FBS-induced apoptosis involved oxidative stress in SCM1 cells, the levels of intracellular ROS including superoxide anion (O_2^-) and hydrogen peroxide (H_2O_2) in *m*-3M3FBS-treated cells were measured by flow cytometry using DHE and DCFH-DA fluorescent dyes, respectively. It was found that 25 and 50 μM *m*-3M3FBS treatment elevated the intracellular levels of O_2^- but decreased the level of H_2O_2 (Fig. 7).

Discussion

Our data suggest that *m*-3M3FBS evoked an immediate $[Ca^{2+}]^i$ rise followed by a slow decline in Ca^{2+}-containing medium. In neutrophils (1), *m*-3M3FBS was shown to induce a spiky $[Ca^{2+}]_i$ rise, and a slowly rising $[Ca^{2+}]_i$ in SH-SY5Y cells. In SH-SY5Y cells, $[Ca^{2+}]_i$ rise was caused solely by Ca^{2+} release from stores, whereas our data show that removal of extracellular Ca^{2+} partially reduced the *m*-3M3FBS-induced $[Ca^{2+}]_i$ rise suggesting contribution from both Ca^{2+} entry and Ca^{2+} release. In SH-SY5Y cells, it was shown that U73122 strongly inhibited *m*-3M3FBS-mediated Ca^{2+} release; in contrast, our data show that U73122 did not change *m*-3M3FBS-induced $[Ca^{2+}]_i$ rise. Thus the effects of *m*-3M3FBS on $[Ca^{2+}]_i$ and the underlying pathways may vary among different cell types.

M-3M3FBS induced concentration-dependent $[Ca^{2+}]_i$ rise in gastric cancer cells between 5 μM and 50 μM. Removal of extracellular Ca^{2+} reduced the *m*-3M3FBS-induced response throughout the measurement period, suggesting that Ca^{2+} influx occurred during the whole stimulation interval. The Ca^{2+} signal was followed by a decay suggesting that the elevated Ca^{2+} was quickly buffered, pumped out of the cells or sequestered by organelles.

The Ca^{2+} sources of *m*-3M3FBS-induced $[Ca^{2+}]_i$ was explored and it was shown that *m*-3M3FBS might induce Ca^{2+} influx *via* evoking store-operated Ca^{2+} entry which was a Ca^{2+} influx pathway induced by depletion of Ca^{2+} stores such as endoplasmic reticulum (24). The traditional L-type Ca^{2+} channel blocker nifedipine was shown to block store-operated Ca^{2+} channels recently (25, 31). Econazole and SK&F96365 are often applied to inhibit store-operated Ca^{2+} entry (17, 26). There is no selective inhibitor so far for this type of Ca^{2+} entry. Aristolochic acid is a phospholipase A2 inhibitor, and was found to inhibit *m*-3M3FBS-induced $[Ca^{2+}]_i$ rise. This suggests that

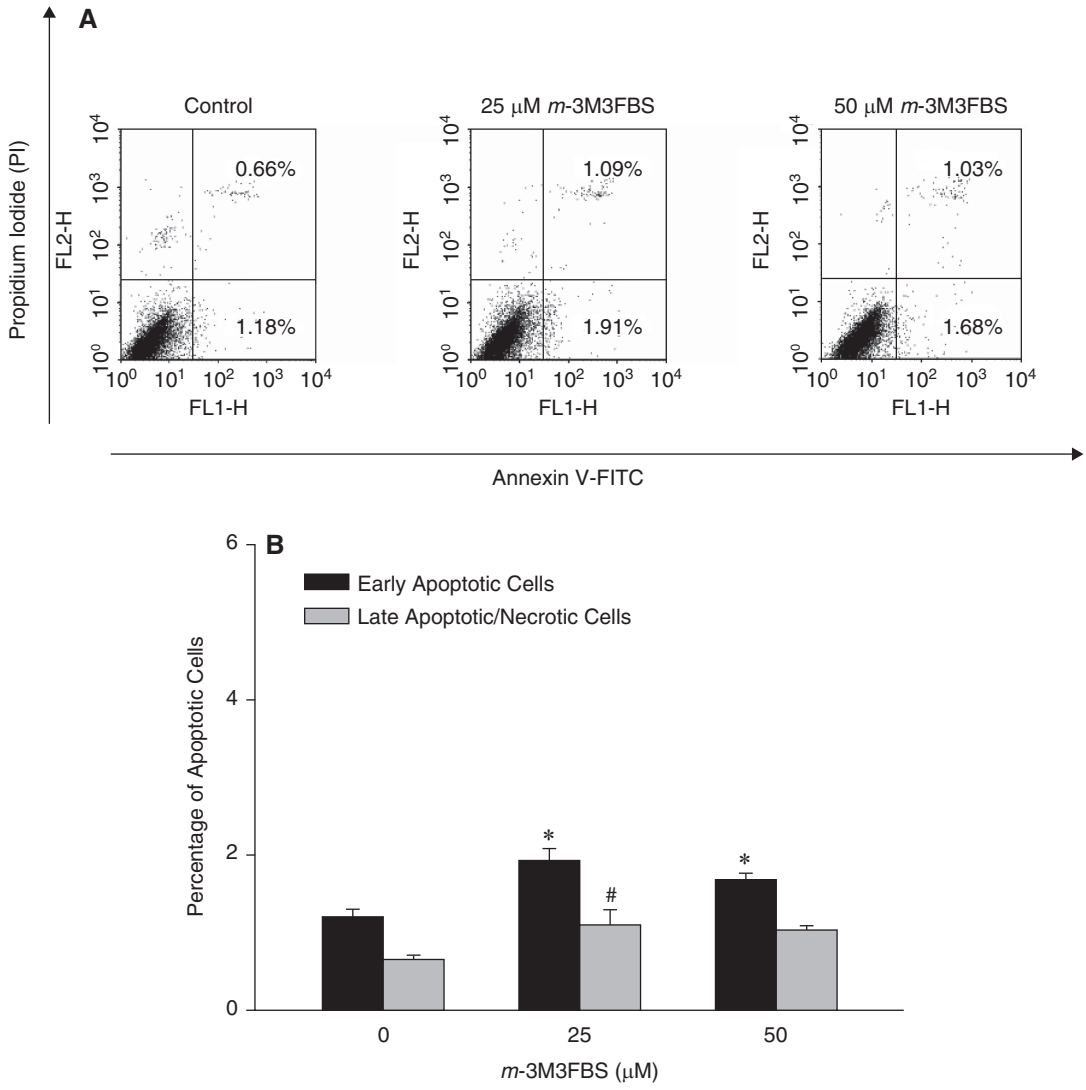

Fig. 6. *M*-3M3FBS-induced apoptosis/necrosis as measured by Annexin V/PI staining. (A) Cells were treated with 0, 25, or 50 μM *m*-3M3FBS, respectively, for 24 h. Cells were then processed for Annexin V/PI staining and analyzed by flow cytometry. (B) The percentage of early apoptotic cells and late apoptotic/necrotic cells. $^{*,\#}P < 0.05$ compared with corresponding control.

phospholipase A2 might participate in *m*-3M3FBS-induced Ca^{2+} signal. Phospholipase A2 was shown to maintain store-operated Ca^{2+} entry in aorta (2) and skeletal muscle fibers (3). The role of protein kinase C in *m*-3M3FBS-induced Ca^{2+} signal was explored because activation of PLC produces IP_3 and diacylglycerol, which activates protein kinase C. Our data show that *m*-3M3FBS-induced $[Ca^{2+}]_i$ rise was decreased by inhibition of protein kinase C activity but not altered by activation of protein kinase C. Thus protein kinase C plays a modulatory role in *m*-3M3FBS-induced response.

The Ca^{2+} stores involved in *m*-3M3FBS-induced Ca^{2+} release were explored. Given that TG treatment reduced a major part of *m*-3M3FBS-induced $[Ca^{2+}]_i$ rise, and treatment with *m*-3M3FBS abolished TG-induced $[Ca^{2+}]_i$ rise, the endoplasmic reticulum stores appear to be the dominant stores. However, TG did not abolish *m*-3M3FBS-induced Ca^{2+} release, thus there are possibly other stores such as NAADP- (6) or cADP-ribose-dependent (15) stores.

One mechanism that underlying Ca^{2+} release from the endoplasmic reticulum is the IP_3-dependent pathway. However, our data suggest that this pathway did not play a role in the Ca^{2+} release, since the Ca^{2+} release was not altered by U73122. *M*-3M3FBS was shown to fail to induce IP_3 formation in SH-SY5Y cells (1). Therefore *m*-3M3FBS was not a selective PLC activator in SCM1 cells.

Our data also suggest that *m*-3M3FBS was cytotoxic to gastric cancer cells in a concentration-dependent fashion. This result is important because many studies use this agent to stimulate PLC without any concern for its possible cytotoxicity. Because *m*-

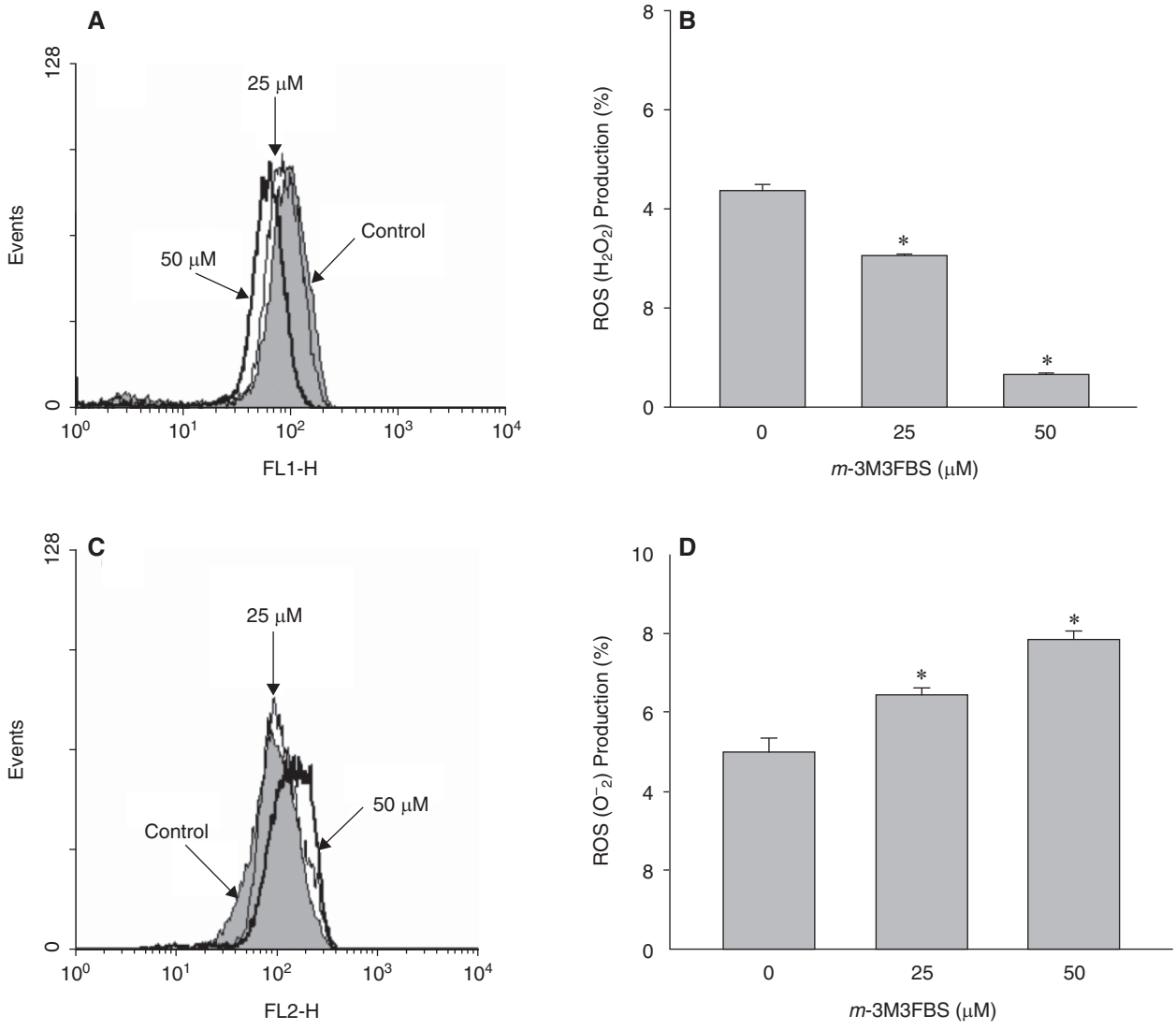

Fig. 7. (A) Effect of *m*-3M3FBS on the hydrogen peroxide level. 2',7'-dichlorofluorescein-diacetate (DCFH-DA) fluorescence was measured after treatment with 0, 25 or 50 μM *m*-3M3FBS in serum-free culture media for 24 h. The fluorescence was quantified using the BD Cell Quest software. Data were means ± SEM of four separate experiments. $*P < 0.05$ compared to control. (B) Effect of *m*-3M3FBS on the superoxide anion level. Dihydroethidine (DHE) fluorescence in cells was measured after treatment with 0, 25 or 50 μM m-3M3FBS in serum-free culture media for 24 h. The fluorescence was quantified using the BD Cell Quest software. Data were means ± SEM of four separate experiments. The data are represented as DCFH-DA (or DHE) fluorescence percentage that refers to cells positive to DCFH-DA (or DHE). Controls are shown in the first column.

3M3FBS induced a $[Ca^{2+}]_i$ rise and cell death, whether these two events were associated was examined. Chelation of cytosolic $[Ca^{2+}]_i$ rise with BAPTA/AM did not prevent *m*-3M3FBS-caused cell death. Thus *m*-3M3FBS-induced $[Ca^{2+}]_i$ rise and cell death were separate events. However, in human renal Caki cancer cells, *m*-3M3FBS was shown to induce apoptosis that was prevented by chelating intracellular Ca^{2+} (18). A logic extension was to explore whether apoptosis was involved *m*-3M3FBS-induced cell death. Annexin/PI staining data suggest that *m*-3M3FBS-induced cell death involved apoptosis. Similarly, *m*-3M3FBS has been shown to induce apoptosis in other cell lines. *m*-3M3FBS was shown to induce apoptosis in tumor cells through caspase activation, down-regulation of XIAP and intracellular Ca^{2+} signaling (18). *M*-3M3FBS also induces monocytic leukemia cell apoptosis (21). Because apoptosis consists of external and internal pathways, the role of ROS (an internal pathway) in *m*-3M3FBS-induced apoptosis was examined. Our results suggest that *m*-3M3FBS at concentrations that evoked $[Ca^{2+}]_i$ rises also increased superoxide levels.

Collectively, the results show that *m*-3M3FBS evoked a $[Ca^{2+}]_i$ rise in SCM1 human gastric cancer cells by inducing Ca^{2+} release from endoplasmic re-

ticulum in a PLC-independent fashion and also by causing Ca^{2+} entry *via* phospholipase A2-, protein kinase C-associated store-operated Ca^{2+} entry pathway. *M*-3M3FBS was not a selective PLC activator in SCM1 cells. This chemical also induced Ca^{2+}-dissociated, ROS-related apoptosis. Increases in $[Ca^{2+}]_i$ can induce diverse cellular responses including apoptosis, enzyme activation, secretion, gene expression, contraction, proliferation, mobility, *etc.*, thus previous researches that applied *m*-3M3FBS to activate PLC might have reported data resulted from effects induced by $[Ca^{2+}]_i$ rise and cytotoxicty, instead of PLC activation. Our study calls for caution of using *m*-3M3FBS in other *in vitro* studies.

Acknowledgments

This work was supported by a grant from Kaohsiung Veterans General Hospital (VGHKS101-019) to CR Jan.

References

1. Bae, Y.S., Lee, T.G., Park, J.C., Hur, J.H., Kim, Y., Heo, K., Kwak, J.Y., Suh, P.G. and Ryu, S.H. Identification of a compound that directly stimulates phospholipase C activity. *Mol. Pharmacol*. 63: 1043-1050, 2003.
2. Boittin, F.X., Petermann, O., Hirn, C., Mittaud, P., Dorchies, O.M., Roulet, E. and Ruegg, U.T. Ca^{2+}-independent phospholipase A_2 enhances store-operated Ca^{2+} entry in dystrophic skeletal muscle fibers. *J. Cell Sci*. 119: 3733-3742, 2006.
3. Boittin, F.X., Gribi, F., Serir, K. and Bény, J.L. Ca^{2+}-independent PLA_2 controls endothelial store-operated Ca^{2+} entry and vascular tone in intact aorta. *Am. J. Physiol. Heart Cir. Physiol*. 295: H2466-H2474, 2008.
4. Bootman, M.D., Berridge, M.J. and Roderick, H.L. Calcium signalling: more messengers, more channels, more complexity. *Cur. Biol*. 12: R563-R565, 2002.
5. Brown, R.A., Leung, E., Kankaanranta, H., Moilanen, E. and Page, C.P. Effects of heparin and related drugs on neutrophil function. *Pulm. Pharmacol. Ther*. 25: 185-192, 2012.
6. Calcraft, P.J., Ruas, M., Pan, Z., Cheng, X., Arredouani, A., Hao, X., Tang, J., Rietdorf, K., Teboul, L., Chuang, K.T., Lin, P., Xiao, R., Wang, C., Zhu, Y., Lin, Y., Wyatt, C.N., Parrington, J., Ma, J., Evans, A.M., Galione, A. and Zhu, M.X. NAADP mobilizes calcium from acidic organelles through two-pore channels. *Nature* 459: 596-600, 2009.
7. Chang, K.H., Tan, H.P., Kuo, C.C., Kuo, D.H., Shieh, P., Chen, F.A. and Jan, C.R. Effect of nortriptyline on Ca^{2+} handling in SIRC rabbit corneal epithelial cells. *Chinese J. Physiol*. 53: 178-184, 2010.
8. Chen, W.C., Cheng, H.H., Huang, C.J., Lu, Y.C., Chen, I.S., Liu, S.I., Hsu, S.S., Chang, H.T., Huang, J.K., Chen, J.S. and Jan, C.R. The carcinogen safrole increases intracellular free Ca^{2+} levels and causes death in MDCK cells. *Chinese J. Physiol*. 50: 34-40, 2007.
9. Cheng, J.S., Lo, Y.K., Yeh, J.H., Cheng, H.H., Liu, C.P., Chen, W.C. and Jan, C.R. Effect of gossypol on intracellular Ca^{2+} regulation in human hepatoma cells. *Chinese J. Physiol*. 46: 117-122, 2003.
10. Chi, C.C., Chou, C.T., Kuo, C.C., Hsieh, Y.D., Liang, W.Z., Tseng, L.L., Su, H.H., Chu, S.T., Ho, C.M. and Jan, C.R. Effect of *m*-3M3FBS on Ca^{2+} handling and viability in OC2 human oral cancer cells. *Acta Physiol. Hung*. 99: 74-86, 2012.
11. Clapham, D.E. Intracellular calcium – Replenishing the stores. *Nature* 375: 634-635, 1995.
12. Dwyer, L., Kim, H.J., Koh, B.H. and Koh, S.D. Phospholipase C-independent effects of 3M3FBS in murine colon. *Eur. J. Pharmacol*. 628: 187-194, 2010.
13. Fang, Y.C., Kuo, D.H., Shieh, P., Chen, F.A., Kuo, C.C. and Jan, C.R. Effect of *m*-3M3FBS on Ca^{2+} movement in Madin-Darby canine renal tubular cells. *Human Exp. Toxicol*. 28: 655-663, 2009.
14. Florenzano, F., Viscomi, M.T., Mercaldo, V., Longone, P., Bernardi, G., Bagni, C., Molinari, M. and Carrive, P. $P2X_2R$ purinergic receptor subunit mRNA and protein are expressed by all hypothalamic hypocretin/orexin neurons. *J. Com. Neurol*. 498: 58-67, 2006.
15. Gerasimenko, J.V., Sherwood, M., Tepikin, A.V., Petersen, O.H. and Gerasimenko, O.V. NAADP, cADPR and IP_3 all release Ca^{2+} from the endoplasmic reticulum and an acidic store in the secretory granule area. *J. Cell Sci*. 119: 226-238, 2006.
16. Grynkiewicz, G., Poenie, M. and Tsien, R.Y. A new generation of Ca^{2+} indicators with greatly improved fluorescence properties. *J. Biol. Chem*. 260: 3440-3450, 1985.
17. Ishikawa, J., Ohga, K., Yoshino, T., Takezawa, R., Ichikawa, A., Kubota, H. and Yamada, T. A pyrazole derivative, YM-58483, potently inhibits store-operated sustained Ca^{2+} influx and IL-2 production in T lymphocytes. *J. Immunol*. 170: 4441-4449, 2003.
18. Jung, E.M., Lee, T.J., Park, J.W., Bae, Y.S., Kim, S.H., Choi, Y.H. and Kwon, T.K. The novel phospholipase C activator, *m*-3M3FBS, induces apoptosis in tumor cells through caspase activation, down-regulation of XIAP and intracellular calcium signaling. *Apoptosis* 13: 133-145, 2008.
19. Kang, Y.H. and Shin, H.M. *Cinnamomi ramulus* ethanol extract exerts vasorelaxation through inhibition of Ca^{2+} influx and Ca^{2+} release in rat aorta. *Evid. Based Complement Alternat. Med*. 2012: 513068, 2012.
20. Krjukova, J., Holmqvist, T., Danis, A.S., Akerman, K.E.O. and Kukkonen, J.P. Phospholipase C activator *m*-3M3FBS affects Ca^{2+} homeostasis independently of phospholipase C activation. *Brit. J. Pharmacol*. 143: 3-7, 2004.
21. Lee, Y.N., Lee, H.Y., Kim, J.S., Park, C., Choi, Y.H., Lee, T.G., Ryu, S.H., Kwak, J.Y. and Bae, Y.S. The novel phospholipase C activator, *m*-3M3FBS, induces monocytic leukemia cell apoptosis. *Cancer Lett*. 222: 227-235, 2005.
22. Liu, S.I., Huang, C.C., Huang, C.J., Wang, B.W., Chang, P.M., Fang, Y.C., Chen, W.C., Wang, J.L., Lu, Y.C., Chu, S.T., Chou, C.T. and Jan, C.R. Thimerosal-induced apoptosis in human SCM1 gastric cancer cells: activation of p38 MAP kinase and caspase-3 pathways without involvement of $[Ca^{2+}]_i$ elevation. *Toxicol. Sci*. 100: 109-117, 2007.
23. Morita, T., Okada, M., Hara, Y. and Yamawaki, H. Mechanisms underlying impairment of endothelium-dependent relaxation by fetal bovine serum in organ-cultured rat mesenteric artery. *Eur. J. Pharmacol*. 668: 401-406, 2011.
24. Putney, J.W. Jr. A model for receptor-regulated calcium entry. *Cell Calcium.* 7: 1-12, 1986.
25. Quinn, T., Molloy, M., Smyth, A. and Baird, A.W. Capacitative calcium entry in guinea pig gallbladder smooth muscle *in vitro*. *Life Sci*. 74: 1659-1669, 2004.
26. Shideman, C.R., Reinardy, J.L. and Thayer, S.A. γ-Secretase activity modulates store-operated Ca^{2+} entry into rat sensory neurons. *Neurosci. Lett*. 451: 124-128, 2009.
27. Thastrup, O., Cullen, P.J., Drøbak, B.K., Hanley, M.R. and Dawson, A.P. Thapsigargin, a tumor promoter, discharges intracellular Ca^{2+} stores by specific inhibition of the endoplasmic reticulum Ca^{2+}-ATPase. *Proc. Natl. Acad. Sci. USA* 87: 2466-2470, 1990.
28. Thompson, A.K., Mostafapour, S.P., Denlinger, L.C., Bleasdale, J.E. and Fisher, S.K. The aminosteroid U-73122 inhibits muscarinic receptor sequestration and phosphoinositide hydrolysis in

SK-N-SH neuroblastoma cells. A role for Gp in receptor compartmentation. *J. Biol. Chem*. 266: 23856-23862, 1991.
29. Tsai, J.Y., Shieh, P., Kuo, D.H., Chen, F.A., Kuo, C.C. and Jan, C.R. Effect of *m*-3M3FBS on Ca^{2+} movement in PC3 human prostate cancer cells. *Chinese J. Physiol*. 53: 151-159, 2010.
30. Tsien, R.Y. New calcium indicators and buffers with high selectivity against magnesium and protons: design, synthesis, and properties of prototype structures. *Biochemistry* 19: 2396-2404, 1980.
31. Young, R.C., Schumann, R. and Zhang, P. Nifedipine block of capacitative calcium entry in cultured human uterine smooth-muscle cells. *J. Soc. Gynecol. Invest*. 8: 210-215, 2001.